

1 Post-flooding disturbance recovery promotes carbon capture 2 in riparian zones

3 Yihong Zhu^{1,3,4#}, Ruihua Liu^{1,3#}, Huai Zhang¹, Shaoda Liu², Zhengfeng Zhang¹, Feihai Yu⁵,
4 Timothy G. Gregoire³

5
6 ¹ School of Earth and Planetary, University of Chinese Academy of Sciences, Beijing, 100049, China

7 ² State Key Laboratory for Water Environment Simulation, School of Environment, Beijing Normal University,
8 Beijing, 100875, China

9 ³ Yale School of the Environment, Yale University, New Haven, 06511, USA

10 ⁴ Department of Environmental Science, Policy and Management, University of California, Berkeley, 94704,
11 USA

12 ⁵ Institute of Wetland Ecology & Clone Ecology; Zhejiang Provincial Key Laboratory of Plant Evolutionary
13 Ecology and Conservation, Taizhou University, Taizhou, 318000, China

14 #Yihong Zhu and Ruihua Liu contributed equally to this paper.

15 *Correspondence to:* Shaoda Liu (liushaoda@bnu.edu.cn); Huai Zhang (h Zhang@ucas.ac.cn)

16
17 **Abstract.** Vegetation, water, and carbon dioxide have complex interactions on carbon mitigation in vegetation-
18 water ecosystems. As one of the major global change drivers of carbon sequestration, flooding disturbance is
19 a fundamental but poorly discussed topic to date. The aquatic and associated riparian systems are highly
20 dynamic vegetation-water carbon capture systems driven by fluvial processes such as flooding. However, their
21 global carbon offset potential is largely unknown. This study examines daily CO₂ perturbations under flooding
22 disturbance in the river (fluvial area) and associated riparian areas with two-year in-situ observations along the
23 Lijiang River. We find that, though the submerged riparian area behaved as a carbon source during the flooding
24 season (CO₂ flux: 2.790 g·m⁻² d⁻¹), the riparian area and the fluvial area as a whole transformed from a carbon
25 source in pre-flooding season (1.833 g·m⁻² d⁻¹) to a carbon sink after recovery in post-flooding season (-0.592
26 g·m⁻² d⁻¹). The fluvial area sequestered carbon (-0.619 g·m⁻² d⁻¹) in post-flooding season instead of releasing
27 carbon as in pre-flooding season (2.485 g·m⁻² d⁻¹). Also, the carbon sequestration capacity of the riparian area
28 was enhanced in post-flooding season (pre-flooding season: -0.156 g·m⁻² d⁻¹, post-flooding season: -0.500 g·m⁻²
29 d⁻¹). We suggest post-disturbance recovery of riparian vegetation played a vital role in this transformation,
30 due to its stronger carbon uptake capacity after recovery from the flooding disturbances. The findings shed
31 light on the quantitative modelling of the riparian carbon cycle under flooding disturbance and underlined the
32 importance of the proper restoration of riparian systems to achieve global carbon offset.

33 1 Introduction

34 Climate change issues stemming from anthropogenic carbon emissions have strengthened dramatically,
35 threatening ecosystem stability and biodiversity (Li et al., 2022; Wang et al., 2020). The increasing atmospheric
36 CO₂ originating from fossil fuel combustion and industrial activities can be regulated by plant metabolism

37 (photosynthesis and respiration) and soil microbial activities (Zheng et al., 1998). In general, the net carbon
38 emission strongly depends on the balance between the production and consumption processes in the vulnerable
39 natural ecosystem (Pugh et al., 2019).

40

41 Aquatic and riparian systems are highly dynamic systems linked by fluvial processes (e.g.: flooding and
42 deposition of alluvial soil) (Naiman and Decamps, 1997; Steiger et al., 2005). Riparian zones are generally
43 defined as complex terrestrial assemblages of plants and other organisms adjacent to an aquatic environment.
44 For instance, the interface between aquatic and terrestrial environments in coniferous forests forms a narrow
45 riparian zone (Gregory et al., 1991). Riparian zones are of great importance in carbon cycling, which is
46 associated with the production and consumption of CO₂ and methane (CH₄) (Zhang et al., 2016; Allen et al.,
47 2007; Liu et al., 2021).

48

49

50 Riparian zone is often considered as sink for CO₂ through photosynthetic assimilation of CO₂ in atmosphere,
51 but disturbance may turn it from carbon sink to carbon source. Seasonal periodic flooding is one of the most
52 common environmental disturbances in riparian zones. Floods can be natural, but human activity such as
53 the construction of dams increasingly causes controlled floods (Darrel Jenerette and Lal, 2005; Dynesius
54 and Nilsson, 1994). Flooding disturbance strongly influences the biotic characteristics of riparian assemblages
55 (Anderson et al., 2020) as well as the carbon cycle. Flooding could increase soil respiration and enzymatic
56 degradation rate (Wilson et al., 2011). It was found that the rate of CO₂ emission in riparian wetlands is higher
57 than that in neighbouring hillslope grasslands (Anderson et al., 2020). Liu et al. (2021) demonstrated that high
58 plant and soil respiration in riparian wetlands lead to larger amounts of CO₂ emission in wet season (335-
59 2790 mg·m⁻² h⁻¹) than in dry season (72 - 387 mg·m⁻² h⁻¹) (Liu et al., 2021). Also, the short-term anaerobic
60 conditions caused by flooding may increase the production of methane because of the strengthened
61 methanogenesis in riparian soils (Hassanzadeh et al., 2019; Hondula et al., 2021; Morse et al., 2012; Le Mer
62 and Roger, 2001; Thorp et al., 2006).

63

64 The influence of flooding disturbance would also depend on the flooding characteristics and the properties of
65 riparian soils. Hirota et al. (2007) found that temporal variations of the greenhouse gases fluxes were strongly
66 manipulated by water-level fluctuations in the sandy shore and by soil temperature in the salt marsh. The
67 duration of flooding was also considered an important factor for riparian carbon dynamics and microbial
68 community structure (Wilson et al., 2011). The spatial heterogeneity of soil properties would also affect the
69 composition and diversity of bacterial communities in riparian zones and thus may influence the riparian carbon
70 cycle under flooding disturbance (Wang et al., 2019b; Wilson et al., 2011).

71

72 Strong seasonality for different greenhouse gas emissions has been detected in previous studies (Gaughan and
73 Waylen, 2012; Allen et al., 2007). With flooding disturbance, riparian vegetation plays an indispensable role
74 in sequestering carbon (Maraseni and Mitchell, 2016) and the variations in riparian vegetation communities are
75 expected to define the ecological role of riparian zones in carbon cycle. During flooding season, flooding

76 submergence may impede gas diffusion and decrease light intensity, leading to high mortality and limited
77 growth of plant species (Colmer et al., 2009). This raises the possibility of elevated carbon (including methane
78 and carbon dioxide) emissions and reduced carbon sequestration from riparian zones, shifting the role of
79 riparian zones from a carbon sink to a carbon source. Conversely, as riparian species adapt to flooding
80 submergence and recover from flooding, riparian zones may gradually return to the initial status or even
81 promote CO₂ capture. Previous studies found that riparian vegetation may increase their leaf gas exchange in
82 response to submergence stress so as to cope with oxygen limitation (Huang et al., 2017; Mommer et al., 2006;
83 Liu et al., 2020). Besides, inundation depth increased reed density, height, leaf area index and biomass, and
84 thus decreased the global warming potential during the growing season (Zhao et al., 2020). Therefore, riparian
85 zone may oscillate between carbon source and sink depending on flooding. It raises the open question of
86 whether riparian zones quantitatively promote or hinder carbon capture overall.

87

88 Riparian zones are believed to have considerable potential to contribute to biodiversity, carbon sequestration,
89 and several other ecosystem services. As a traditional practice, riparian vegetation has been cleared for crop
90 and pasture production in numerous places worldwide, leading to increases in greenhouse gas emissions
91 (Maraseni and Cockfield, 2011). It is noteworthy that proper and efficient restoration of the riparian zones is
92 fundamental for the proper functioning of riparian ecosystem services. Thus, it has been listed as a priority in
93 the IPCC community (Bullock et al., 2011). However, the current research on the riparian carbon sequestration
94 under flooding disturbance remains poorly constrained. There has been some modelling work about the riparian
95 carbon stock, but fewer on the carbon flux. For instance, Dybala et al., (2019) modelled the change in carbon
96 stock as a function of vegetation age, considering effects of climate and whether or not the riparian forest had
97 been actively planted (Dybala et al., 2019). One limitation for models like Riparian Ecosystem Management
98 Model (REMM) or other riparian models is that they require a large amount of site specific parameters, many
99 of which are often modeled using other models as inputs (Vidon et al., 2019). In addition to climatic factors,
100 factors such as floodplain width, flow regime, frequency of inundation, and the presence of dams, diversions,
101 and levees also need to be considered when modelling the riparian carbon flux with the disturbance of flooding
102 (Sutfin et al., 2016).

103

104 In order to figure out how floods affect the balance between carbon emission and sequestration in riparian areas,
105 we quantified the vertical CO₂ fluxes at the soil-air interface (riparian are) and water-air interface (fluvial area)
106 during the flooding season and non-flooding seasons (pre-flooding season and post-flooding season) based on
107 two-year in-situ measurements along the Lijiang River. Considering an overall small contribution of CH₄ to
108 the carbon balance of riparian zones (Liu et al., 2021; Vidon et al., 2019), only CO₂ fluxes were measured in
109 analysis. We establish that a riparian system promotes carbon capture despite enhanced carbon releases during
110 flooding periods and its capacity is directly related to the resilience and post-disturbance recovery of riparian
111 vegetation. We suggest that promoting the recovery of riparian systems and establishing high flooding-tolerant
112 vegetation coverage is key to promoting carbon capture in the context of increasing flood risks under climate
113 change.

114 **2 Methods**

115 **2.1 In-situ observation setup**

116 Our study site is in the downstream of the 164 kilometres long Lijiang River in the Pearl River Basin in
117 northwestern Guangxi Zhuang Autonomous Province, Southwest China (25° 06' N, 110° 25'; Fig. A1). Lijiang
118 River has a typical karst landscape, with widely exposed carbonate rocks (Wang et al., 2019b). The river from
119 Guilin to Yangshuo is the most typical karst development area. The river channel is composed of sand and
120 pebbles, and the soil type is red loam with high sand content (Wang et al., 2019b). This area experiences a
121 monsoon-based humidity subtropical climate, where the mean annual rainfall is 1900 mm, and the annual
122 temperature ranges from 7.9 °C to 28.0 °C. In the dry season (normally September to March next year), the
123 minimum daily average flow discharge is often below 20 m³/s. Therefore, drought stress profoundly influences
124 the early-stage development of riparian species. By contrast, in the flooding season (April to August),
125 discharges over 1000 m³/s are common during flood events, inner islands are completely submerged, and some
126 riparian species cease to grow or are destroyed. The soils of the Lijiang River riparian zone are sand-based,
127 with sand contents ranging from 74.99% to 88.44%; silt and clay contents are lower, accounting for
128 approximately 10% (Wang et al., 2019b; Lu and Wang, 2015). With the decrease of inundation frequency, the
129 sand content is found to decrease while the clay and silt content increased gradually (Wang et al., 2019b). Soil
130 pH is around 6.99 to 7.71, and soil total nitrogen is around 0.93 to 1.40 (g·kg⁻¹) (Wang et al., 2019b). Different
131 vegetation zones can further influence the chemical properties of soils (Lu and Wang, 2015).

132 **2.2 Experiment design**

133 **2.2.1 Gas collection**

134 Four transects were established on one island downstream of the Lijiang River (Fig. A1). The distance between
135 each transect was approximately 3 m. Four subplots spaced 5-8 m apart were deployed in each transect,
136 perpendicular to the waterlines and extended from the edge of the water body to the upper area. Site selection
137 and chamber placement minimized differences in the microclimate among chamber stations. CO₂ in four 50 x
138 50 cm subplots along each transect were sampled by static chamber techniques. Four static chambers were used
139 at each site (Fig. A1). Chambers were positioned in the same location for the monitoring phase. On the river,
140 floating static chambers were used (Sun et al., 2012) and were set up on shallow water and deep water. The
141 floating static chamber was a cylindrical chamber (of radius 50cm and height 65cm) with a floating ring (about
142 20cm) around the bottom of the chamber to keep it floating on the water, and was thus sealed by the water. On
143 the land during non-flooding seasons, the terrestrial static chambers (length 50 cm, width 50 cm, and height 50
144 cm) were used and were set up on riparian areas with vegetation and without vegetation. The terrestrial static
145 chamber was put on a stainless-steel underside base (length 50 cm, width 50 cm and height 15 cm) instead of
146 setting directly on the ground. The underside base increased the chamber's size and prevented damage to the
147 vegetation inside (Sun et al., 2013). There was a groove on the top of the underside base, and the upper portion
148 of chamber was designed to be put into this groove. By adding water to the groove, the whole setting was sealed
149 (Sun et al., 2012, 2013). The floating static chamber and the terrestrial static chamber both were covered by
150 foam and reflective aluminium, which can easily reflect the heat from sunlight and thus prevent rapid

151 temperature changes or temperature becoming too high in the chamber (Søvik and Kløve, 2007). Also, the
152 chambers contained two exhaust fans, a thermometer and a tube inside. A syringe was used to collect gas
153 samples from the tube at intervals of 0, 10, 20 and 30 minutes. For 24-hour monitoring, samples were taken
154 every 4 hours (a total 6 times per day starting at 10:00 and finishing at 06:00 the next day) in one day in April,
155 August, and October (covering pre-flooding season, flooding season, and post-flooding season) in 2014 (both
156 riparian area and river) and 2016 (river). In other words, diel data was taken at the 0, 10min 20min and 30min
157 of 10:00, 14:00, 18:00, 22:00, 2:00 and 6:00.

158 **2.2.2 Determination of CO₂ flux and hydro-environment conditions**

159 Gas samples were collected by a syringe from the tube of chamber and were instantly transferred to airtight
160 glass bottles (20ml, Agilent5190-2286). All samples were analysed within three days. The CO₂ concentration
161 was measured using gas chromatography (Agilent7890A) equipped with an electron capture detector (ECD)
162 and a flame ionization detector (FID) (Agilent Technologies, 2010). The measurements were conducted by
163 Pony Testing International Group Co. Ltd (300887:CH). Standard CO₂ gases (with concentration of 0 and
164 10000 pm, respectively) were used for method calibration. The calculation formula of CO₂ flux is

$$165 \quad F = \frac{M}{V_0} \frac{P}{P_0} \frac{T_0}{T} H \frac{dc}{dt} \quad (1)$$

166 where F represents the gas flux ($\mu\text{g}\cdot\text{m}^{-2}\text{h}^{-1}$), M is the molar mass, V_0 represents the normal state of molar
167 volume (22.4 L/mol), P_0 and T_0 are the pressure and temperature of the standard conditions (1013.25 hPa,
168 273.15 K) for gases, and d_c/d_t is the slope of the regression curve as gas concentration variable with time,
169 respectively. The height of the chamber (H , cm), in-situ air pressure (P , hPa), and air temperature (T , K) were
170 recorded during the sampling as well. The all-day CO₂ flux was calculated by integrating the diel CO₂ flux of
171 different measuring times. The environmental information, including total organic carbon (TOC) and total
172 inorganic carbon (TIC) downstream (Yangshuo Gauge) of the Lijiang River, was also recorded. Meanwhile,
173 the water level was recorded hourly during the experiment period.

174 **2.2.3 Vegetation inventory and flooding tolerant experiment**

175 Vegetation inventory was conducted by three 15 m x 5 m transects along with this field site. Coverage, number
176 of ramets, and height are measured. After the field inventory, about 300 seeds of *C. aciculatus*, which was the
177 dominant riparian species after flooding, were sown in planting trays filled with peat (Pindstrup Seeding;
178 Pindstrup Mosebrug A/S, Pindstrup, Denmark). Seeds were bought from Forest Science Co, Ltd. of Beijing
179 Forestry University. Eight grass plants with one single ramet were transplanted in the experimental pots. In
180 total, 178 ramets with similar sizes of each species were selected for the experiment, of which 18 were randomly
181 used to obtain their initial length and dry mass, and the remaining 80 ramets were used for the experiments.
182 The initial ramet length of *C. aciculatus* was 9.56 ± 0.18 cm, and the dry mass was 38.56 ± 5.36 mg. The
183 experiment lasted three months, from August 01 to November 01. The mean temperature and relative humidity
184 were 26.21 ± 0.33 °C and $59.02 \pm 1.46\%$, respectively. Sufficient tap water was added to each container to
185 maintain the plant submerged in the water. At harvest, new ramets produced by each initial one were
186 interconnected by aboveground stolon, so we could harvest and measure the growth attributes of plants in each
187 treatment separately. We counted the number of ramets and weighed each plant's dry leaf, rhizome, and biomass

188 in each container. All plant parts were oven-dried at 70°C for 72 h before weighing. The collection of materials
189 complied with relevant institutional, national, and international guidelines and legislation.

190 **2.2.4 Annual riparian and river CO₂ emission calculation**

191 We are interested in whether or under what conditions the riparian area and the fluvial area as a whole can
192 achieve carbon neutralization (which means the net carbon emission is zero) at the annual level with flooding
193 disturbance. We take flooding disturbance into account by dividing the whole year into pre-flooding season,
194 flooding season, and post-flooding season. We assume that flooding events happen at an annual timescale and
195 consider the time that flooding would happen as flooding season. The occurrence of extreme weather like
196 rainstorms or frost is not considered here. Here, we define riparian area as the area that would be submerged
197 during the flooding season but exposed during non-flooding seasons. Fluvial area refers to the river in non-
198 flooding seasons and the river plus the flooded riparian area during the flooding season. Field investigation
199 showed that the riparian area makes up 25% of the whole river width (riparian plus fluvial) and the vegetation
200 coverage is about 60%. Thus, the annual riparian CO₂ emission is calculated as the sum of emissions in pre-
201 flooding season, flooding season and post-flooding season by the following equation:

202

$$203 \quad C_{annual} = \sum C_{i,j} = \sum W_{i,j} * D_j * a_{i,j} \quad (2)$$

204 Where C_{annual} is the annual expected carbon emission ($C_{annual} = 0$ means the whole region reaches carbon
205 neutralization at the annual level), $C_{i,j}$ is the annual CO₂ emission of fluvial or riparian area in different seasons
206 ($i=1, 2$ refer to fluvial and riparian area respectively, $j=1, 2, 3$ refer to pre-flooding season, flooding season,
207 and post-flooding season respectively), $W_{i,j}$ is the width of fluvial area or riparian area in different seasons, D_j
208 is the number of days of corresponding season, and $a_{i,j}$ is the all-day CO₂ flux of fluvial area or riparian area in
209 different seasons. Specially, during flooding season, the width of riparian area ($W_{1,2}$) is 0 meter because all the
210 riparian area is submerged. The all-day CO₂ flux of riparian area in pre- ($a_{2,1}$) or post-flooding season ($a_{2,3}$) is
211 calculated by the following equation:

$$212 \quad a = a_{veg} * p + a_{soil} * (1 - p) \quad (3)$$

213 Where a_{veg} is the all-day CO₂ flux of vegetation area, a_{soil} is the CO₂ flux of bare soil area, and p is the vegetation
214 coverage.

215 **2.2.5 Data analysis**

216 For riparian areas, two-way repeated-measurement ANOVA was employed to examine the effects of vegetation
217 (with vegetation vs. without vegetation; between-subject factor) and time (measuring times in one day, within-
218 subject factor) on the CO₂ flux in two sampling stages (April: pre-flooding and October: post-flooding). For
219 fluvial areas, two-way repeated-measurement ANOVA was used to examine the effects of sampling position
220 (with vegetation vs. without vegetation or under water surface; between-subject factor) and time (measuring
221 times in one day; within-subject factor) on CO₂ flux in sampling stages (April: pre-flooding, August: during
222 flooding, and October: post-flooding). The p -values were calculated with the null hypothesis that the CO₂ flux
223 of riparian area or fluvial area is not influenced by the factors mentioned. Before analyses, homogeneity of
224 variance and normality are also examined. All data analyses were performed by the SPSS statistical software

225 package (<https://www.ibm.com/products/spss-statistics>, version 22.0, Chicago, IL, USA). The effects were
226 considered significant if p -value < 0.05 .
227

228 3 Results

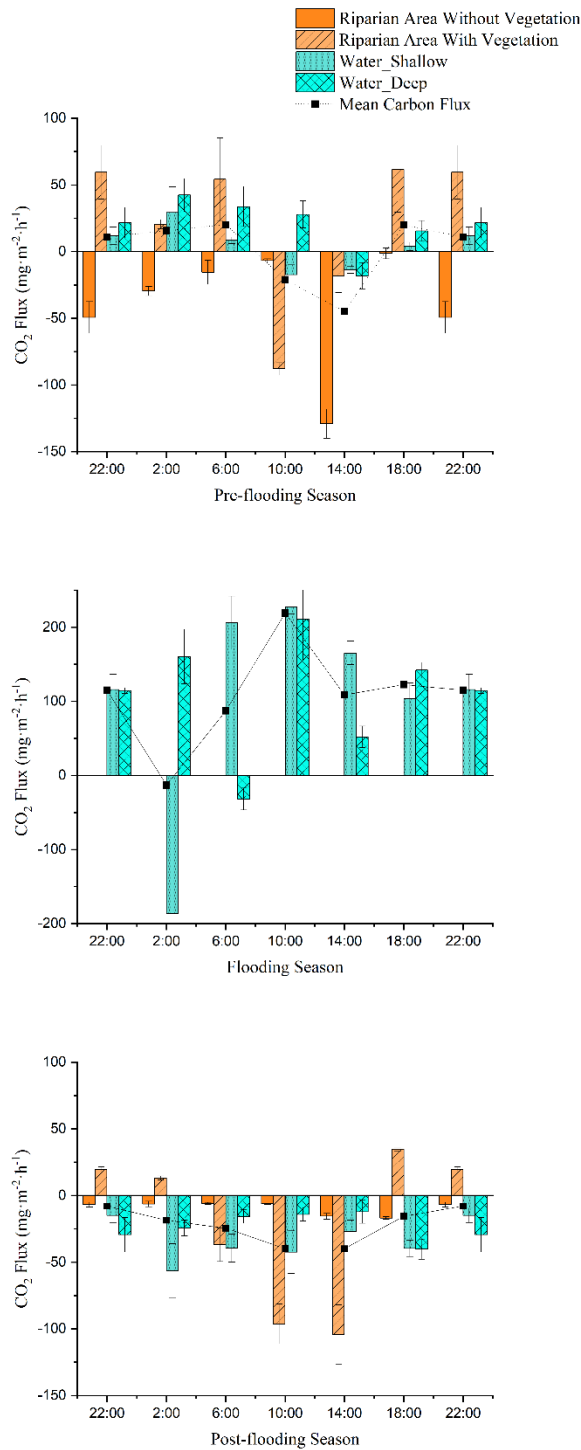
229 3.1 Vegetation overall promotes carbon capture despite a weak carbon release during the pre-flooding 230 nights

231 We assume that diel CO₂ flux follows similar patterns as measured on the selected days during the pre-flooding
232 and post-flooding season. Based on this assumption, we compared the diel CO₂ flux of pre-flooding season and
233 post-flooding season. In order to evaluate the effect of vegetation on riparian CO₂ flux, we directly measured
234 the CO₂ fluxes in the riparian area with and without vegetation (bare soil) in different seasons.
235

236 Significant diel variations in CO₂ fluxes were observed in the riparian area in both pre-flooding season (April:
237 low water level before flooding) and post-flooding season (October: resumed low water level after flooding;
238 Table A1). Within a day, the carbon sequestration in the riparian area with vegetation peaked at 10:00 in April
239 and at 14:00 in October (April: $-87.89 \text{ mg}\cdot\text{m}^{-2}\text{h}^{-1}$; October: $-104.33 \text{ mg}\cdot\text{m}^{-2}\text{h}^{-1}$); and the maximum carbon
240 emission occurred at 18:00 (April: $61.49 \text{ mg}\cdot\text{m}^{-2}\text{h}^{-1}$; October: $34.75 \text{ mg}\cdot\text{m}^{-2}\text{h}^{-1}$; Fig. 1). However, the time
241 periods that the riparian area with vegetation functions as a carbon sink differed in pre-flooding and post-
242 flooding season. In April, carbon sequestration in the riparian area with vegetation was observed between 10:00
243 to 14:00 hours; while in October, the carbon sequestration was observed between 6:00 to 14:00 hours (Fig. 1).
244 Thus, in post-flooding season, the riparian area with vegetation sequestered carbon for a longer time. Indeed,
245 the vegetation area's all-day CO₂ flux was $0.358 \text{ g}\cdot\text{m}^{-2}\text{d}^{-1}$ in April but was $-0.680 \text{ g}\cdot\text{m}^{-2}\text{d}^{-1}$ in October,
246 transferring from a carbon source to a carbon sink at the daily level.
247

248 Since the flux of vegetated area included fluxes from both soils below and the vegetation above, we subtracted
249 the CO₂ flux of bare soil from the CO₂ flux of vegetated area to measure how the cover of vegetation improve
250 or reduce the carbon sequestration. In April, the difference between area with and without vegetation was 0.128
251 $\text{g}\cdot\text{m}^{-2}\text{d}^{-1}$, indicating that vegetation cover actually reduced carbon sequestration and contributed to carbon
252 emission. In October, the difference was $-0.453 \text{ g}\cdot\text{m}^{-2}\text{d}^{-1}$, indicating that the capacity of vegetation to fix carbon
253 improved after submergence.
254

255 The riparian area is composed of vegetated area and bare soil area. During the field investigation, we found the
256 vegetation coverage in Lijiang riparian area is about 60%. Using vegetation coverage as the weight, we can get
257 the accumulated CO₂ flux of riparian area (Section 2.2.4, equation (3)). Within a day, the carbon sequestration
258 in the riparian area peaked at 14:00 (April: $-62.680 \text{ mg}\cdot\text{m}^{-2}\text{h}^{-1}$; October: $-68.813 \text{ mg}\cdot\text{m}^{-2}\text{h}^{-1}$), and the maximum
259 carbon emission occurred at 18:00 (April: $36.347 \text{ mg}\cdot\text{m}^{-2}\text{h}^{-1}$; October: $14.110 \text{ mg}\cdot\text{m}^{-2}\text{h}^{-1}$; Fig. 1). In both April
260 and October, the all-day carbon fluxes in the riparian area were negative, indicating that the riparian area acted
261 as a carbon sink in non-flooding season (April: $-0.156 \text{ g}\cdot\text{m}^{-2}\text{d}^{-1}$, October: $-0.500 \text{ g}\cdot\text{m}^{-2}\text{d}^{-1}$). The carbon uptake
262 in October, which represented the post-flooding season, was higher. Overall, we found that in the post-flooding



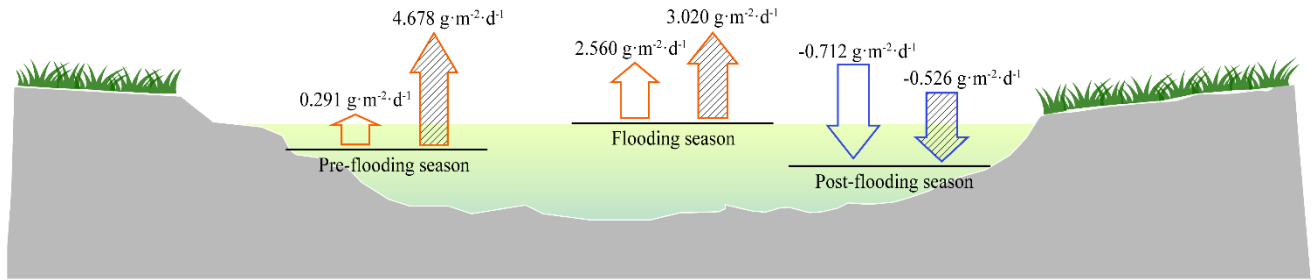
season, the riparian vegetation can sequester CO₂ for a longer time and fix a higher amount of carbon. Thus, even though the all-day CO₂ flux of bare soil changed from -0.927 g·m⁻² d⁻¹ to -0.231 g·m⁻² d⁻¹, showing a reduced capacity of carbon sequestration after flooding, the whole riparian area still turned out to be a carbon sink in the post-flooding season. **Figure 1.** CO₂ fluxes in riparian area (with vegetation and without vegetation) and fluvial area (shallow area with vegetation and deep area without vegetation) during pre-flooding season (measured in April), flooding season (August), and post-flooding season (October).

3.2 Flooding causes transient carbon emission in fluvial area which turns to sequester carbon during post-flooding season

During the flooding, the riparian areas with and without vegetation were submerged, so only the carbon fluxes from the fluvial areas (water-air interfaces) were measured (Fig.1b). The water-air CO₂ flux is calculated as the mean of the CO₂ flux in deep water and shallow water considering their coverage is almost half and half. Significant diel variations in CO₂ fluxes were also observed in fluvial area ($p < 0.01$), but the CO₂ fluxes from shallow water and deep water did not have significant differences ($p > 0.05$; Table A2). By analysing and calculating the all-day CO₂ flux, we found that the fluvial area turned from carbon sources in pre-flooding season and during flooding season to a carbon sink in post-flooding season. In

296 carbon sources before and during flooding, with a CO₂ flux ranging from 0.291 g·m⁻² d⁻¹ to 4.678 g·m⁻² d⁻¹ (Fig.
 297 2). However, after flooding, the river became a carbon sink (Fig. 2). Thus, after flooding, both the riparian area
 298 and the fluvial area turned out to be a carbon sink.
 299

300 Based on the vegetation coverage and the ratio of riparian area width to river width in flooding season, we can
 301 accumulate the CO₂ flux of riparian area and the fluvial area as a whole (Section 2.2.4). The CO₂ flux of the
 302 whole region was 1.833 g·m⁻²·d⁻¹ in pre-flooding season, and -0.592 g·m⁻²·d⁻¹ in post-flooding season, which
 303 indicated that the whole region turned from a carbon source to a carbon sink after flooding.
 304



305
 306 **Figure 2.** All-day CO₂ flux with low water-level in pre-flooding season, high water-level during flooding
 307 season, and resumed low water-level in post-flooding season in 2014 (Blank) and 2016 (Dashed). The upward
 308 arrow refers to carbon emission, and the downward arrow refers to carbon uptake.
 309

310 **3.3 Flooding transiently decreases vegetation diversity and promotes the establishment of new dominant**
 311 **species**

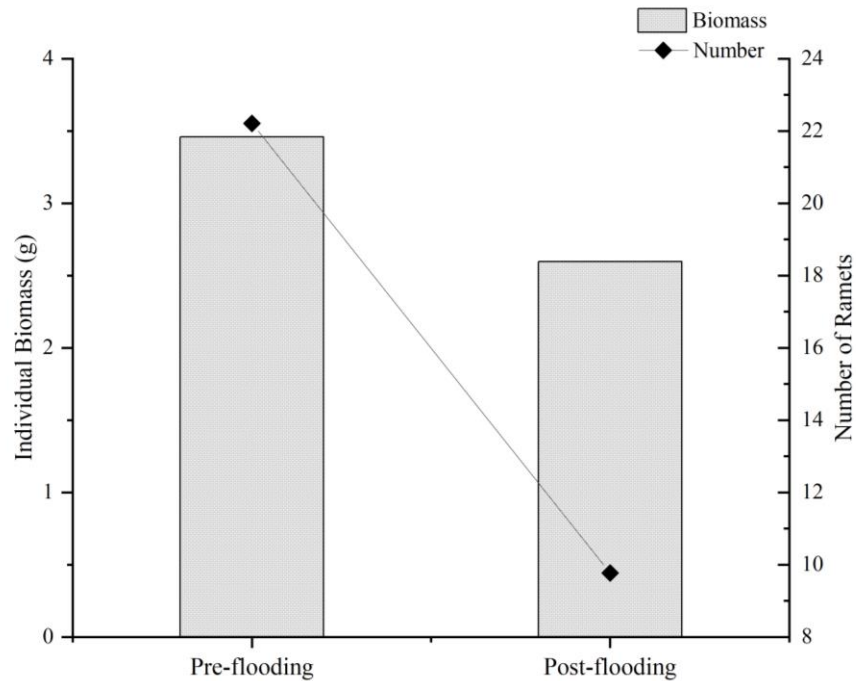
312 Vegetation plays an essential role in the carbon sequestration of riparian area. We hypothesize that the
 313 established riparian vegetation species differed, which leads to different vegetation-related carbon fluxes
 314 between the pre- and post-flooding periods. We observed that species richness was severely disturbed after
 315 flooding. The species richness index decreased from 2.945 in pre-flooding season to 1.695 in post-flooding
 316 season (Table 1, Table A3). The dominant species also changed. In pre-flooding season, *Cynodon dactylon*
 317 (Linn.) Pers. was dominant, having wide distribution and high coverage in the riparian areas. In post-flooding
 318 season, *Chrysopogon aciculatus* (Retz.) Trin. (*C. aciculatus*) and *Polygonum lapathifolium* L. were prevalent
 319 in surviving species (Table 1). In the 90-day submergence-controlled experiment, *C. aciculatus* also survived,
 320 showing good tolerance of flooding submergence, though both individual biomass and the total number of *C.*
 321 *aciculatus* decreased (Fig. 3).
 322

323 **Table 1** The species richness and dominant species change from pre-flooding season to post-flooding season.

	Average species number	Species richness index	Dominant species	Average coverage of dominant species (%)
Pre-flooding	13	2.945	<i>Cynodon dactylon</i>	28.61
Post-flooding	7	1.695	<i>Chrysopogon aciculatus</i>	28.75

324 Note: The species number listed here is the average number by plots. The whole list of plant species can be
325 found in Table

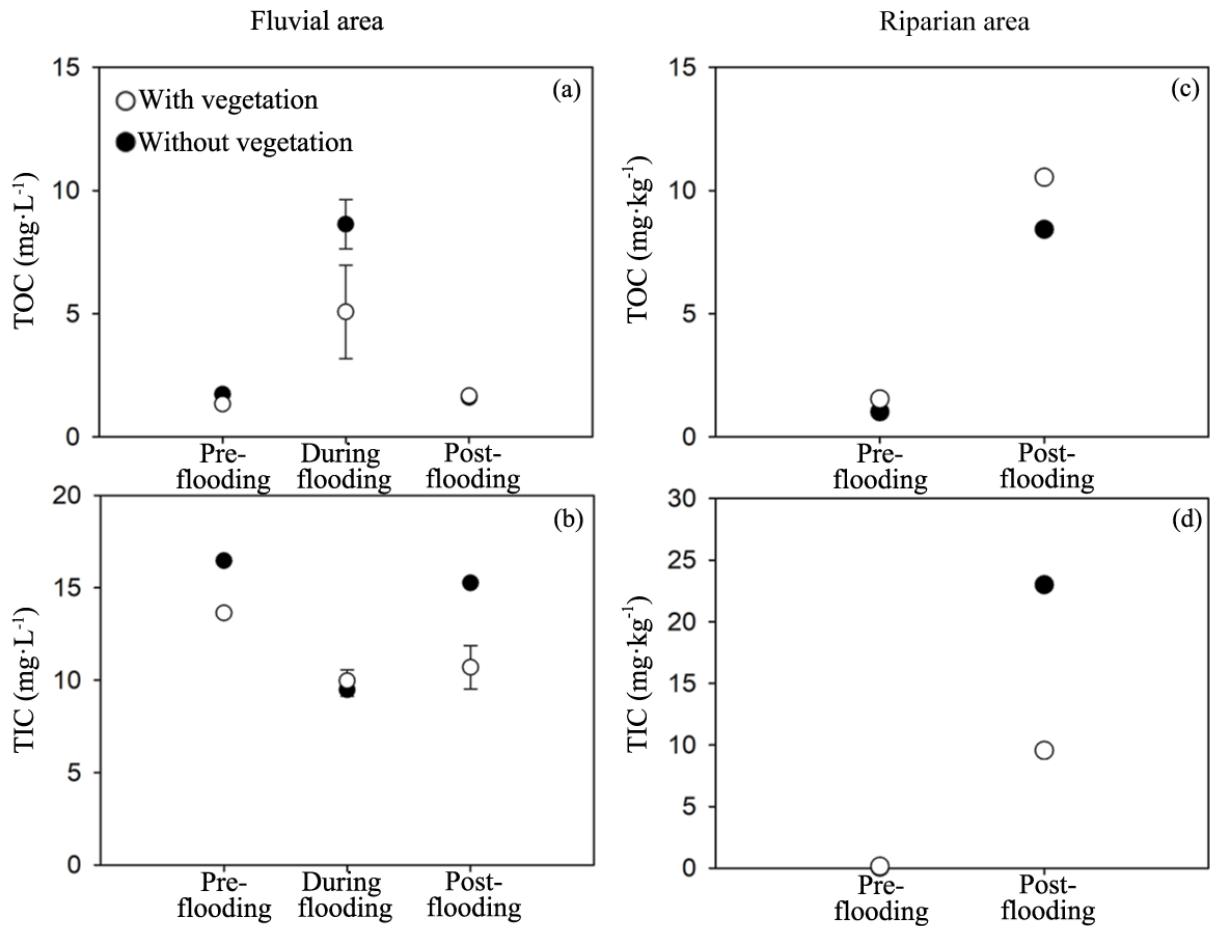
326 A3.



337
338
339 **Figure 3.** The comparison of the individual biomass and number of *Chrysopogon aciculatus* before and after
340 flooding in the controlled experiment.

341 3.4 Vegetation density defines carbon sequestration capacity in riparian habitats

342 We measured total organic carbon (TOC) and total inorganic carbon (TIC) in riparian soils and the fluvial area
343 during different periods. TOC and TIC displayed different patterns across seasons. TOC in fluvial area was
344 substantially higher during the flooding period than that during the pre- and post-flooding seasons (Fig. 4a;
345 $p < 0.001$, Table A4), probably due to a higher mobilization of riparian organic carbon to the river during the
346 flooding period. This is in consistence with an enrichment effect for organic carbon under high discharge
347 (Raymond and Saiers, 2010). In contrast, TIC in fluvial area was in lower concentration during the flooding
348 season than during the pre- and post-flooding seasons (Fig. 4b; $p < 0.001$, Table A4). In addition to a dilution
349 effect for TIC by high discharge during the flooding period, this also suggests a stronger effect of riparian area
350 on fluvial carbon during the non-flooding seasons than during flooding periods. Additionally, we show that
351 both TOC and TIC in riparian soils were substantially higher during the post-flooding season than during the
352 pre-flooding season (Fig. 4c, d; $p < 0.001$ Table A4), suggesting a higher carbon sequestration capacity for
353 riparian vegetation after recovery from flooding disturbances.



354
 355 **Figure 4.** Total organic carbon (TOC) and total inorganic carbon (TIC) in the study area. The fluvial area and
 356 riparian area include study areas with vegetation and without vegetation. TOC and TIC were also measured in
 357 different sampling stages. The ANOVA results for habitats, season, and interaction effects are given, including
 358 the degree of freedom (*df*), *F*, and *P* values in Appendix Table A4.
 359

360 **4 Discussion**

361 The present work demonstrates significant variations in spatial and temporal carbon fluxes from riparian zones
 362 of the Lijiang River. In April, the all-day CO₂ fluxes in 2014 and 2016 were positive on the daily scale in fluvial
 363 area, indicating a net emission from fluvial area of the river to the atmosphere. However, opposite results were
 364 found for the CO₂ flux in October after the flooding disturbance, which was negative and indicated a capacity
 365 for carbon sequestration. In the riparian area, the vegetation was found to promote the overall carbon
 366 sequestration and keep the riparian area as a carbon sink. It demonstrates that the carbon sequestration capacity
 367 of a given system depends strongly on the post-disturbance recovery of riparian vegetation.

368 **4.1 Increased carbon emission during flooding periods of the riparian zone**

369 Hydrological flow has been found to be an essential factor within the carbon cycle of riparian ecosystems
370 (Zarnetske et al., 2018). Our data suggest that flooding not only affects carbon emission from the fluvial channel
371 but also the carbon fluxes of the riparian area. With regard to carbon emission from the fluvial area, our data
372 show that carbon emission of water-air interface significantly increased and showed a net emission of CO₂ in
373 both the daytime and night-time (all-day CO₂ flux: 0.291 g·m⁻² d⁻¹ in April, 2.560 g·m⁻² d⁻¹ in August). This is
374 probably due to the increased lateral carbon flux from terrestrial areas to rivers due to flooding. Research found
375 that when water flows through ecosystem, it would pick up dissolved organic carbon from vegetation and soils,
376 transporting the carbon from riparian ecosystem to streams (Raymond and Saiers, 2010). A large amount of
377 carbon could be transported to the river because of enhanced hydrological connectivity between the fluvial
378 channel and its riparian areas during flooding periods (Zarnetske et al., 2018).

379

380 When comparing the CO₂ flux of shallow-water area (with aquatic vegetation) and deep-water area (without
381 vegetation) (Fig. A2), it is also found that shallow-water released less carbon in pre-flooding season and
382 captured more carbon in post-flooding season than deep-water area. However, during the flooding season, both
383 the shallow-water and deep-water areas uptake carbon, probably because of an enhanced input of carbon from
384 riparian vegetation and soils to the fluvial channel.

385

386 In addition to increased hydrologic connectivity between the riparian area and fluvial channel of the river,
387 enhanced carbon emission also results from enhanced substrate availability during flooding (Hirota et al., 2007).
388 Previous work also reported that the extensive root system of riparian species with strong taproots and well-
389 developed fibrous roots could force the species to demand more oxygen and accelerate root respiration and
390 CO₂ emissions from the neighbouring rhizosphere (Elias et al., 2015). In submerged areas, the CO₂ may be
391 transported to water and then released to the atmosphere as the carbon flux of water surface. Especially, the
392 recovery of some C₄ riparian species after periodic flooding also contributed to the higher gas transportability
393 and abundant substrate for CO₂ emission compared to the performance of C₃ species (Still et al., 2003). In
394 addition to riparian vegetation, inundation could also increase the decomposition of stored organic matter
395 (Denef *et al.*, 2001, Marín-Muñiz *et al.*, 2015) and soil respiration (Anderson *et al.*, 2020, Ou *et al.*, 2019). A
396 previous study found that after 25 days of soil moisture enhancement, the anaerobiosis stimulates CO₂ loss by
397 1.5 times more than the normal soil moisture environment (Huang & Hall, 2017). Flooding leads to elevated
398 soil moisture for weeks or even months, and thus an accelerated CO₂ supply to the inundated channel.

399

400 **4.2 Post-disturbance survived vegetation as a critical factor for riparian systems to sequester carbon**

401 We observed that the carbon sequestration of riparian area and fluvial area as a whole was greatly enhanced
402 after the flooding period, to the point that the overall carbon flux was negative. In consistence with our analysis,
403 Kathilankal et al. (2008) proposed that tidal inundation caused a mean reduction of 49 % in the marsh-
404 atmosphere carbon (CO₂) flux compared to non-flooded conditions (Kathilankal *et al.*, 2008). Our study offers

405 proof that the hydrological flow is a determining factor on whether the riparian ecosystem is a net carbon source
406 or sink.

407

408 One possible reason is that the vegetation's recovery after flooding enhances its ability to sequester more CO₂
409 for photosynthesis. The post-flooding succession of vegetation suggests that not all riparian plants can survive
410 submergence and to become efficient carbon sinks. Indeed, species richness decreased after flooding, which
411 indicates a decrease of the interspecific competition, giving a chance to species that can quickly recover from
412 submergence. The dominant species changed from *C. dactylon* to *C. aciculatus* after flooding disturbance.
413 Although the individual biomass and number of DOCC. *aciculatus* did not increase, existing literature suggests
414 that the leaf maximum net photosynthesis rate may increase significantly after severe submergence in the
415 riparian zones of Lijiang (Huang *et al.*, 2017, Jie *et al.*, 2012). For the clonal plants, its physiological integration
416 allowing them to survive submergence and spread rapidly after de-submergence. Luo *et al.* (2014), studying
417 *Alternanthera philoxeroides* (alligator weed) after 30 days of submergence, found that connections between
418 submerged and non-submerged ramets enhance the performance of the submerged ramets; and the de-
419 submerged ramets had high soluble sugar concentrations, suggesting high metabolic activities (Luo *et al.*, 2014).
420 Wei *et al.* (2018) also found that after 30 days of submergence, stolon connection significantly increased growth,
421 biomass allocation to roots and photosynthetic capacities of the submerged ramets, and increased growth and
422 photosynthetic capacities of the unsubmerged ramets (Wei *et al.*, 2018). Also, flooding could promote CO₂ use
423 efficiency and the ability of the plant to use low light (Wang *et al.*, 2019a). The enhanced photosynthetic
424 capacity is believed to be one of the physiological strategies for species growing in critical zones with flooding
425 disturbance. Moreover, human impacts can no longer be ignored on the riparian ecosystem (Ren *et al.*, 2019),
426 suggesting vegetation that can recover quickly and densely is essential to allow riparian zones to be efficient
427 carbon sinks.

428

429 Our results suggest, on an annual scale, riparian area behaves either as a net source or sink of carbon depending
430 on the relative importance between enhanced emission during flooding and the strength of post-disturbance
431 carbon absorbance. Assuming the carbon flux rates of flooding season and non-flooding seasons were the same
432 as we have measured on the selected days (Section 2.2.4, Fig.1-2), we estimated that the riparian area and the
433 fluvial area as a whole can achieve carbon neutralization ($C_{annual}=0$) only when flooding days are fewer than
434 15 days. Therefore, the relative ratio of flooding to non-flooding days are essential factors to determine whether
435 the riparian area is a net source or sink on an annual scale, and future long-term, high-frequency measurements
436 are required to monitor the carbon dynamics of the riparian zone. Also, besides the contribution of recovered
437 vegetation, our data shows that bare soil also contributes to the carbon neutralization, but the mechanism for
438 bare soil to capture carbon still needs further analysis.

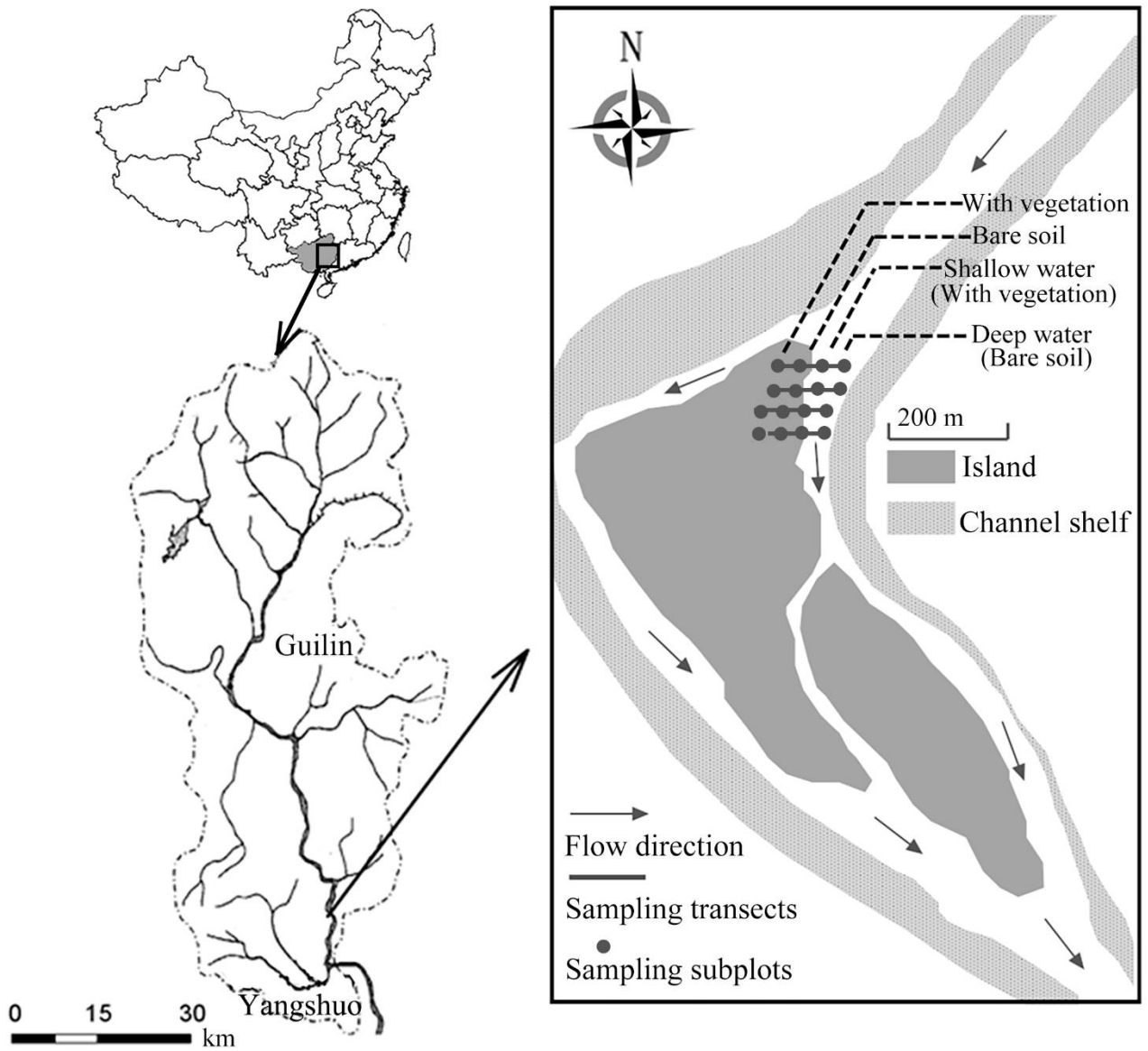
439

440 Nowadays, the risk and the number of global flooding events are expected to rise significantly with climate
441 changes (Hirabayashi *et al.*, 2013). This means that the annual carbon cycle of riparian area and fluvial area as
442 a whole is subject to a more variant and stronger impact from flooding. Previous research found that with a
443 warmer climate, there would be a large increase in flood frequency in Southeast Asia, Peninsular India, eastern

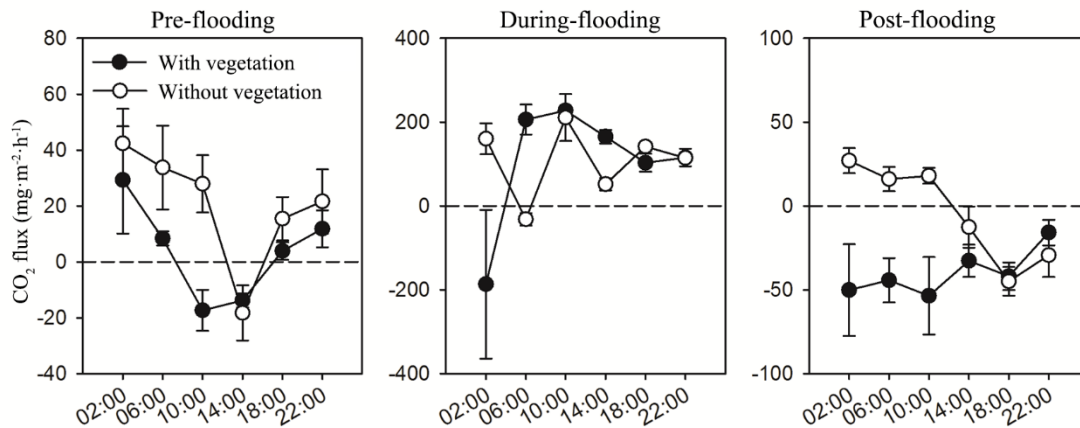
444 Africa and the northern half of the Andes (Hirabayashi et al., 2013). Our research highlights that flooding
445 disturbance would not only cause large carbon emission during the flooding season, but can also promote
446 carbon sequestration in the post-flooding season. It is therefore necessary to consider the dynamic effect of
447 flooding on ecosystems' carbon cycle especially under global climate change.
448

449 **5 Conclusions**

450 Under climate change, both the risk and the number of flooding event are rising. Our analysis reinforces the
451 need to consider post-disturbance recovered vegetation in riparian zone as a climate mitigation strategy. The
452 recovery of survived riparian vegetation from flooding disturbance can limit overall carbon emission and help
453 neutralize the carbon emissions caused by flooding. Flooding also improves the resource hunting ability of
454 water area, which turns the riparian zone from a carbon source to a carbon sink. This study highlights that
455 carbon-conscious conservation efforts in post-flooding season should promote the establishment of high
456 densities of specific plant species that are both flooding-resistant and efficient at capturing carbon.



458
 459 **Appendix Figure A1:** The location of the study site in the island downstream of Lijiang River in Guilin city,
 460 southwest China (25° 06' N, 110° 25' E). There were four sampling transects (black lines), each spaced 3 m,
 461 and four subplots (black squares) were arranged in each transect, with the distance of 5-8 m between each other.
 462
 463



464

465 **Appendix Figure A2:** Effects of time (measuring times in one day) on CO₂ flux in the water-air surface of the
 466 fluvial area with vegetation (shallow-water, filled) and without vegetation (deep-water, blank) in the three
 467 sampling stages. Mean ± 1 SE is given.

468

469

470 **Appendix Table A1.** Repeated measurements ANOVA for effects of vegetation (riparian areas with vegetation
 471 vs. without vegetation; between-subject factor) and time (measuring times in one day; within-subject factor)
 472 on the CO₂ fluxes in two sampling stages (April and October) in riparian areas. Degree of freedom, *F*, and *P*
 473 (significance) values.

Sampling stages	Effects	df	<i>F</i>	<i>p</i> -value
April	Vegetation (V)	1,8	102.506	<0.001
	Time (T)	5,40	22.411	<0.001
	T x V	5,40	12.909	<0.001
October	Vegetation (V)	1,8	61.47	<0.001
	Time (T)	5,40	9.25	<0.001
	T x V	5,40	5.959	<0.001

474

F value: the ratio of two estimates of the variance between or within groups in ANOVAs;

475

P-value: the probability of the *F* value in the *F* distribution. The *p*-values were calculated under the null
 476 hypothesis that CO₂ flux is not influenced by the existence of vegetation or measuring times in riparian areas.

477

478

479

480 **Appendix Table A2.** Repeated measurements ANOVA for effects of vegetation (shallow area with vegetation
 481 vs. deep area without vegetation; between-subject factor) and time (measuring times in one day; within-subject
 482 factor) on CO₂ fluxes in three sampling stages (April, August, and October) in fluvial areas. Degree of freedom
 483 (*df*), *F*, and *P* (significance) values are given.

Sampling stages	Effects	<i>df</i>	<i>F</i>	<i>p</i> -value
-----------------	---------	-----------	----------	-----------------

April	Vegetation(V)	1,4	0.003	0.956
	Time (T)	5,20	4.306	0.008
	T x P	5,20	7.431	<0.001
August	Vegetation(V)	1,4	0.003	0.956
	Time (T)	5,20	4.306	0.008
	T x P	5,20	7.431	<0.001
October	Vegetation(V)	1,4	7.484	0.052
	Time (T)	5,20	2.183	0.097
	T x P	5,20	6.552	0.001

484 *F* value: the ratio of two estimates of the variance between or within groups in ANOVAs; *P*-value: the
485 probability of the *F* value in *F* distribution. The *p*-values were calculated under the null hypothesis that CO₂
486 flux is not influenced by vegetation or measuring times in fluvial areas.

487

488 **Appendix Table A3.** The whole plant species in pre-flooding season (surveyed in April) and post-flooding
 489 season (surveyed in October).

Pre-flooding season	Post-flooding season
<i>Aster tataricus</i>	<i>Alternanthera philoxeroides</i>
<i>Astragalus sinicus</i>	<i>Aster tataricus</i>
<i>Athyrium sinense</i>	<i>Astragalus sinicus</i>
<i>Cardamine hirsuta</i>	<i>Cardamine hirsuta</i>
<i>Carex duriuscula</i> subsp. <i>stenophylloides</i>	<i>Carex polycephala</i> var. <i>simplex</i>
<i>Carex polycephala</i> var. <i>simplex</i>	<i>Chrysopogon aciculatus</i>
<i>Chrysopogon aciculatus</i>	<i>Cynodon dactylon</i>
<i>Cichorium endivia</i>	<i>Oxalis corymbosa</i>
<i>Conyza canadensis</i>	<i>Polygonum hydropiper</i>
<i>Cynodon dactylon</i>	<i>Polygonum lapathifolium</i>
<i>Digitaria ciliaris</i>	<i>Stellaria media</i>
<i>Hemarthria altissima</i>	
<i>Lindernia antipoda</i>	
<i>Oxalis corymbosa</i>	
<i>Poa annua</i>	
<i>Polygonum hydropiper</i>	
<i>Polygonum lapathifolium</i>	
<i>Polygonum muricatum</i>	
<i>Potentilla chinensis</i>	
<i>Salvia plebeia</i>	
<i>Stellaria media</i>	
<i>Urena lobata</i>	
<i>Viola philippica</i>	
<i>Vitex negundo</i>	

490

491

492 **Appendix Table A4** ANOVA results for effects of vegetation (with vegetation vs. without vegetation;
 493 between-subject factor), sampling seasons (pre-flooding, during flooding, post-flooding), and interaction
 494 effects on total organic carbon (TOC) and total inorganic carbon (TIC) in two positions (fluvial area vs. riparian
 495 area). Degree of freedom (*df*), *F*, and *P* (significance) values are given.

	Fluvial area				Riparian area			
	TOC		TIC		TOC		TIC	
	<i>F</i> _{1,8}	<i>P</i>	<i>F</i> _{1,8}	<i>P</i>	<i>F</i> _{1,8}	<i>P</i>	<i>F</i> _{1,8}	<i>P</i>
Vegetation	3.3	0.094	25.8	<0.001	116.8	<0.001	2289.3	<0.001
Sampling stage	24.2	<0.001	46.6	<0.001	4515.9	<0.001	13360.4	<0.001
Interaction	2.5	0.0120	10.7	<0.001	42.8	<0.001	2336.7	<0.001

496 **Data Availability**

497 Correspondence and requests for data should be addressed to Huai Zhang (hzhang@ucas.ac.cn).

Author contributions

500 RL conceived, designed the study and collected the data with FY. YZ analysed the data, completed data visualization. YZ and RL wrote the original manuscript. HZ, SL, TGG reviewed and edited the manuscript. HZ acquired funding and resources for this study.

Competing interests

The authors declare that they have no conflict of interest.

Disclaimer

505 Publisher's note: Copernicus Publications remains neutral with regard to jurisdictional claims in published maps and institutional affiliations.

Funding

This research is supported by the National Science Foundation of China (41725017). It is also partially supported by the Strategic Priority Research Program (B) of the Chinese Academy of Sciences (XDB18010202).

510 **Acknowledgements**

We are grateful to the fishermen Qiaolian Huang, Yuhua Chen, and Fengzhan Xu along the Lijiang River for their assistance in the overnight field sampling. We also thank Songlin Liu and Maolin Gan at South China Sea Institute of Oceanology, Chinese Academy of Sciences, for supporting TIC and TOC measurements.

References

515 Agilent Technologies: User Manuals Agilent 7890A Gas Chromatograph Operating Guide, 2010.

Allen, D. E., Dalal, R. C., Rennenberg, H., Meyer, R. L., Reeves, S., and Schmidt, S.: Spatial and temporal variation of nitrous oxide and methane flux between subtropical mangrove sediments and the atmosphere, *Soil Biology and Biochemistry*, 39, 622–631, <https://doi.org/10.1016/j.soilbio.2006.09.013>, 2007.

- 520 Anderson, N. J., Heathcote, A. J., Engstrom, D. R., and Globocarb data contributors: Anthropogenic alteration of nutrient supply increases the global freshwater carbon sink, *Sci. Adv.*, 6, eaaw2145, <https://doi.org/10.1126/sciadv.aaw2145>, 2020.
- Bullock, J. M., Aronson, J., Newton, A. C., Pywell, R. F., and Rey-Benayas, J. M.: Restoration of ecosystem services and biodiversity: conflicts and opportunities, *Trends in Ecology & Evolution*, 26, 541–549, <https://doi.org/10.1016/j.tree.2011.06.011>, 2011.
- 525 Colmer, T. D., Voesenek, L. a. C. J., Colmer, T. D., and Voesenek, L. a. C. J.: Flooding tolerance: suites of plant traits in variable environments, *Functional Plant Biol.*, 36, 665–681, <https://doi.org/10.1071/FP09144>, 2009.
- Darrel Jenerette, G. and Lal, R.: Hydrologic sources of carbon cycling uncertainty throughout the terrestrial-aquatic continuum, *Global Change Biol.*, 0, 1873–1882, <https://doi.org/10.1111/j.1365-2486.2005.01021.x>, 2005.
- Dybala, K. E., Matzek, V., Gardali, T., and Seavy, N. E.: Carbon sequestration in riparian forests: A global synthesis and meta-analysis, *Global Change Biology*, 25, 57–67, <https://doi.org/10.1111/gcb.14475>, 2019.
- 530 Dynesius, M. and Nilsson, C.: Fragmentation and Flow Regulation of River Systems in the Northern Third of the World, *Science*, 266, 753–762, <https://doi.org/10.1126/science.266.5186.753>, 1994.
- Elias, E., Steele, C., Havstad, K., Steenwerth, K., Chambers, J., Deswood, H., Kerr, A., Albert, R., Schwartz, M., Stine, P., and Steele, R.: Southwest Regional Climate Hub and California Subsidiary Hub assessment of climate change vulnerability and adaptation and mitigation strategies, 2015.
- 535 Gaughan, A. E. and Waylen, P. R.: Spatial and temporal precipitation variability in the Okavango–Kwando–Zambezi catchment, southern Africa, *Journal of Arid Environments*, 82, 19–30, <https://doi.org/10.1016/j.jaridenv.2012.02.007>, 2012.
- Gregory, S. V., Swanson, F. J., McKee, W. A., and Cummins, K. W.: An Ecosystem Perspective of Riparian Zones, *BioScience*, 41, 540–551, <https://doi.org/10.2307/1311607>, 1991.
- 540 Hassanzadeh, Vidon, Gold, Pradhanang, and Lowder: RZ-TRADEOFF: A New Model to Estimate Riparian Water and Air Quality Functions, *Water*, 11, 769, <https://doi.org/10.3390/w11040769>, 2019.
- Hirabayashi, Y., Mahendran, R., Koirala, S., Konoshima, L., Yamazaki, D., Watanabe, S., Kim, H., and Kanae, S.: Global flood risk under climate change, *Nature Clim Change*, 3, 816–821, <https://doi.org/10.1038/nclimate1911>, 2013.
- 545 Hirota, M., Senga, Y., Seike, Y., Nohara, S., and Kunii, H.: Fluxes of carbon dioxide, methane and nitrous oxide in two contrastive fringing zones of coastal lagoon, Lake Nakaumi, Japan, *Chemosphere*, 68, 597–603, <https://doi.org/10.1016/j.chemosphere.2007.01.002>, 2007.
- Hondula, K. L., Jones, C. N., and Palmer, M. A.: Effects of seasonal inundation on methane fluxes from forested freshwater wetlands, *Environ. Res. Lett.*, 16, 084016, <https://doi.org/10.1088/1748-9326/ac1193>, 2021.
- 550 Huang, D., Wang, D., Ren, Y., Qin, Y., and Wu, L.: Responses of leaf traits to submergence stress and analysis of the economic spectrum of plant species in an aquatic-terrestrial ecotone, the Li River, *Acta Ecol. Sin.*, 37, <http://dx.doi.org/10.5846/stxb201508281789>, 2017.
- Le Mer, J. and Roger, P.: Production, oxidation, emission and consumption of methane by soils: A review, *European Journal of Soil Biology*, 37, 25–50, [https://doi.org/10.1016/S1164-5563\(01\)01067-6](https://doi.org/10.1016/S1164-5563(01)01067-6), 2001.

- Li, X., Shi, F., Ma, Y., Zhao, S., and Wei, J.: Significant winter CO₂ uptake by saline lakes on the Qinghai-Tibet Plateau, *Global Change Biology*, 28, 2041–2052, <https://doi.org/10.1111/gcb.16054>, 2022.
- 555 Liu, R., Liang, S., Long, W., and Jiang, Y.: Variations in Leaf Functional Traits Across Ecological Scales in Riparian Plant Communities of the Lijiang River, Guilin, Southwest China, *trcs*, 11, <https://doi.org/10.1177/1940082918804680>, 2020.
- Liu, X., Lu, X., Yu, R., Sun, H., Xue, H., Qi, Z., Cao, Z., Zhang, Z., and Liu, T.: Greenhouse gases emissions from riparian wetlands: an example from the Inner Mongolia grassland region in China, *Biogeosciences*, 18, 4855–4872, <https://doi.org/10.5194/bg-18-4855-2021>, 2021.
- 560 Lu, Y. and Wang, D.: Diversity of plants on the Alluvial islands of Lijiang River basin and the physicochemical properties of their soil, *Nature Environment and Pollution Technology*, 14, 533–540, 2015.
- Luo, F.-L., Chen, Y., Huang, L., Wang, A., Zhang, M.-X., and Yu, F.-H.: Shifting effects of physiological integration on performance of a clonal plant during submergence and de-submergence, *Annals of Botany*, 113, 1265–1274, <https://doi.org/10.1093/aob/mcu057>, 2014.
- 565 Maraseni, T. N. and Cockfield, G.: Crops, cows or timber? Including carbon values in land use choices, *Agriculture, Ecosystems & Environment*, 140, 280–288, <https://doi.org/10.1016/j.agee.2010.12.015>, 2011.
- Maraseni, T. N. and Mitchell, C.: An assessment of carbon sequestration potential of riparian zone of Condamine Catchment, Queensland, Australia, *Land Use Policy*, 54, 139–146, <https://doi.org/10.1016/j.landusepol.2016.02.013>, 2016.
- Mommer, L., Lenssen, J. P. M., Huber, H., Visser, E. J. W., and de Kroon, H.: Ecophysiological Determinants of Plant Performance under Flooding: A Comparative Study of Seven Plant Families, *Journal of Ecology*, 94, 1117–1129, 2006.
- 570 Morse, J. L., Ardón, M., and Bernhardt, E. S.: Greenhouse gas fluxes in southeastern U.S. coastal plain wetlands under contrasting land uses, *Ecological Applications*, 22, 264–280, <https://doi.org/10.1890/11-0527.1>, 2012.
- Naiman, R. J. and Decamps, H.: The Ecology of Interfaces: Riparian Zones, *Annual Review of Ecology and Systematics*, 28, 621–658, 1997.
- 575 Pugh, T. A. M., Arneith, A., Kautz, M., Poulter, B., and Smith, B.: Important role of forest disturbances in the global biomass turnover and carbon sinks, *Nat Geosci*, 12, 730–735, <https://doi.org/10.1038/s41561-019-0427-2>, 2019.
- Raymond, P. A. and Saiers, J. E.: Event controlled DOC export from forested watersheds, *Biogeochemistry*, 100, 197–209, <https://doi.org/10.1007/s10533-010-9416-7>, 2010.
- Ren, Y., Wang, D., and Li, X.: Impacts of Human Disturbances on Riparian Herbaceous Communities in a Chinese Karst River, *Nature Environment and Pollution Technology*, 18, 1107–1118, 2019.
- 580 Søvik, A. K. and Kløve, B.: Emission of N₂O and CH₄ from a constructed wetland in southeastern Norway, *Science of The Total Environment*, 380, 28–37, <https://doi.org/10.1016/j.scitotenv.2006.10.007>, 2007.
- Steiger, J., Tabacchi, E., Dufour, S., Corenblit, D., and Peiry, J.-L.: Hydrogeomorphic processes affecting riparian habitat within alluvial channel-floodplain river systems: a review for the temperate zone, *River Res. Applic.*, 21, 719–737, <https://doi.org/10.1002/rra.879>, 2005.
- 585

- Still, C. J., Berry, J. A., Collatz, G. J., and DeFries, R. S.: Global distribution of C₃ and C₄ vegetation: Carbon cycle implications: C₄ PLANTS AND CARBON CYCLE, *Global Biogeochem. Cycles*, 17, 6-1-6-14, <https://doi.org/10.1029/2001GB001807>, 2003.
- 590 Sun, Q., Shi, K., Damerell, P., Whitham, C., Yu, G., and Zou, C.: Carbon dioxide and methane fluxes: Seasonal dynamics from inland riparian ecosystems, northeast China, *Science of The Total Environment*, 465, 48–55, <https://doi.org/10.1016/j.scitotenv.2013.01.036>, 2013.
- Sun, Q.-Q., Whitham, C., Shi, K., Yu, G.-H., and Sun, X.-W.: Nitrous oxide emissions from a waterbody in the Nenjiang basin, China, *Hydrology Research*, 43, 862–869, <https://doi.org/10.2166/nh.2012.060>, 2012.
- 595 Sutfin, N. A., Wohl, E. E., and Dwire, K. A.: Banking carbon: a review of organic carbon storage and physical factors influencing retention in floodplains and riparian ecosystems: BANKING CARBON, *Earth Surf. Process. Landforms*, 41, 38–60, <https://doi.org/10.1002/esp.3857>, 2016.
- Thorp, J. H., Thoms, M. C., and Delong, M. D.: The riverine ecosystem synthesis: biocomplexity in river networks across space and time, *River Research and Applications*, 22, 123–147, <https://doi.org/10.1002/rra.901>, 2006.
- 600 Vidon, P. G., Welsh, M. K., and Hassanzadeh, Y. T.: Twenty Years of Riparian Zone Research (1997–2017): Where to Next?, *Journal of Environmental Quality*, 48, 248–260, <https://doi.org/10.2134/jeq2018.01.0009>, 2019.
- Wang, J., Wang, D., Ren, Y., and Wang, B.: Coupling relationships between soil microbes and soil nutrients under different hydrologic conditions in the riparian zone of the Lijiang River, *Acta Ecol. Sin*, 39, <https://doi.org/10.5846/stxb201803260595>, 2019a.
- 605 Wang, J., Wang, D., and Wang, B.: Soil Bacterial Diversity and its Determinants in the Riparian Zone of the Lijiang River, China, *Current Science*, 117, 1324, <https://doi.org/10.18520/cs/v117/i8/1324-1332>, 2019b.
- Wang, J., Feng, L., Palmer, P. I., Liu, Y., Fang, S., Bösch, H., O’Dell, C. W., Tang, X., Yang, D., Liu, L., and Xia, C.: Large Chinese land carbon sink estimated from atmospheric carbon dioxide data, *Nature*, 586, 720–723, <https://doi.org/10.1038/s41586-020-2849-9>, 2020.
- 610 Wei, G.-W., Shu, Q., Luo, F.-L., Chen, Y.-H., Dong, B.-C., Mo, L.-C., Huang, W.-J., and Yu, F.-H.: Separating effects of clonal integration on plant growth during submergence and de-submergence, *Flora*, 246–247, 118–125, <https://doi.org/10.1016/j.flora.2018.08.004>, 2018.
- Wilson, J. S., Baldwin, D. S., Rees, G. N., and Wilson, B. P.: The effects of short-term inundation on carbon dynamics, microbial community structure and microbial activity in floodplain soil, *River Research and Applications*, 27, 213–225, <https://doi.org/10.1002/rra.1352>, 2011.
- 615 Zarnetske, J. P., Bouda, M., Abbott, B. W., Saiers, J., and Raymond, P. A.: Generality of Hydrologic Transport Limitation of Watershed Organic Carbon Flux Across Ecoregions of the United States, *Geophys. Res. Lett.*, 45, <https://doi.org/10.1029/2018GL080005>, 2018.
- 620 Zhang, T., Huang, X., Yang, Y., Li, Y., and Dahlgren, R. A.: Spatial and temporal variability in nitrous oxide and methane emissions in urban riparian zones of the Pearl River Delta, *Environ Sci Pollut Res*, 23, 1552–1564, <https://doi.org/10.1007/s11356-015-5401-y>, 2016.

Zhao, M., Han, G., Wu, H., Song, W., Chu, X., Li, J., Qu, W., Li, X., Wei, S., Eller, F., and Jiang, C.: Inundation depth affects ecosystem CO₂ and CH₄ exchange by changing plant productivity in a freshwater wetland in the Yellow River Estuary, *Plant Soil*, 454, 87–102, <https://doi.org/10.1007/s11104-020-04612-2>, 2020.

625 Zheng, X., Wang, M., Wang, Y., Shen, R., Li, J., J., H., M., K., Li, L., and Jin, J.: Comparison of manual and automatic methods for measurement of methane emission from rice paddy fields, *Adv. Atmos. Sci.*, 15, 569–579, <https://doi.org/10.1007/s00376-998-0033-5>, 1998.